COMPARATIVE STUDY ON TURBULENT FLOW STRUCTURE UNDER AIR, CO_2 AND SF_6 GAS BLASTING VISUALIZED BY BAND-PASS FILTERING SCHLIEREN SYSTEM

Yuki INADA
Saitama University – Japan
inada@mail.saitama-u.ac.jp

Hiroyuki NAGAI
The University of Tokyo – Japan
nagai_h@hvg.t.u-tokyo.ac.jp

Akiko KUMADA
The University of Tokyo – Japan
kumada@hvg.t.u-tokyo.ac.jp

Kunihiko HIDAKA
The University of Tokyo – Japan
hidaka@hvg.t.u-tokyo.ac.jp

Yuki DEMURA
Kanazawa University – Japan
ydemura@stu.kanazawa-u.ac.jp

Yu TABATA
Kanazawa University – Japan
avatar@stu.kanazawa-u.ac.jp

Yasunori TANAKA
Kanazawa University – Japan
tanaka@ec.t.kanazawa-u.ac.jp

Tomoyuki NAKANO
CRIEPI – Japan
tomoyuki@criepi.denken.or.jp

Mitsuaki MAEYAMA
Saitama University – Japan
maeyama@mail.saitama-u.ac.jp

ABSTRACT

Multi-directional turbulent structures were visualized for gas-blasted arc discharges under current-zero phases generated in a 50-mm-long interelectrode gap confined by a model gas flow nozzle, in order to conduct a systematic comparison of turbulent gas dynamics among three kinds of different arc-quenching gas media: air, CO_2 and SF_6. The turbulence of all gases demonstrated hierarchical structures, where small turbulence in sizes of ~10 μm were distributed circularly and formed millimeter-scale large circles. The small turbulence in dimensions of 33-43 μm was even stronger for SF_6, compared with air and CO_2. Further, the electron density imaging was complementally conducted in order to investigate the correlation between the turbulent dynamics and the electron density decaying process. The electron density for SF_6 demonstrated the fastest decrease, which was followed by CO_2 and air. A combination of the turbulent and electron density behavior suggested that the strongest small turbulence of SF_6 could cause the cold gas mixing into the arc, which resulted in the rapid arc cooling and the fastest electron density reduction.

INTRODUCTION

The realization of green electric power networks requires the replacement and reduction of the SF_6 gas extensively used in high voltage gas circuit breakers [1]. Here, the current interruption performance of the gas circuit breakers is largely dependent on the electron density of the decaying arc in the current-zero phase [2-4]. Therefore, systematic comparison of the electron densities among various kinds of arc-quenching gas media is a promising approach for the effective search and development of the SF_6-alternative gases and for the optimized use of these eco-friendly gases [5].

A large number of simulation studies have been conducted for many arc-quenching gases [6, 7] and it has been widely considered that the chemical and thermal non-equilibriums and thermodynamic transport properties play important roles in the electron density decaying process. However, our detailed experimental research has been recently demonstrating that the electron density decaying process can not be fully explained by the two non-equilibriums and thermodynamic transport properties; rather, it can be dominated by the turbulent dynamics of the blasted gas media [8]. Although the detailed observation of the turbulent dynamics is crucially important for the realization of the environmentally compatible gas circuit breakers, there is no accessible experimental data on the quenching gas dependence of the turbulent structures, such as the sizes and shapes.

While the gas dynamics coupled with the circuit-breaker-related arcs has been extensively measured by several imaging techniques mainly including Shadowgraph method [9], pulsed holography [10] and differential interferometry [11], turbulent behaviour has been best observed by Schlieren optics [12]. However, a simple Schlieren method implementing a knife edge [13] is only applicable for hydrodynamic phenomena with unidirectional medium density gradients. Therefore, such a typical Schlieren technique is not suitable for the detailed observation of the complex turbulent structures having the multi-directional gas density variations.

In this study, the multi-directional turbulent structures with certain sizes were selectively visualized with sufficient spatiotemporal resolution by developing a specialized Schlieren method. In addition to the turbulent visualization, two-dimensional electron density imaging was also conducted by using the Shack-Hartmann sensors in order to investigate the correlation between the turbulent dynamics and the electron density decaying process in the nozzle throat region, which has been reported to determine the current interruption performance of the gas circuit breakers. These diagnostic techniques were applied to gas-blasted air, CO_2 and SF_6 arc discharges under current-zero phases of an AC 1400-A arc current.

EXPERIMENT

The present Schlieren method implemented a spatial filter,

instead of the conventional knife edge. Fig.1 shows a schematic illustration of the spatial filter used in this study. The spatial filter was composed of a pair of lenslets and a bandpass plate with a circular aperture. The bandpass plate was arranged in the confocal plane of the two lenslets. The laser wavefront transmitting through one lenslet is spatially Fourier transformed in the confocal plane [14]. Therefore, the low spatial frequency components are collected in the central region of the bandpass plate, while the high spatial frequency components of the laser wavefront are distributed in the outer region of the bandpass plate. Thus, the specified spatial frequency components can penetrate the circular aperture selectively. The spatial filter operates as a bandpass filter for the laser wavefront. Since the laser wavefont transmitting through an arc region has information on the spatial frequency of the turbulent gas density, the spatial filter enables us to extract the turbulent structure with a certain spatial frequency, i.e. a specified dimension.

Assuming that the positive ions included in arc plasma are only univalent, a change in refractive indexes between before and after plasma generation ΔN is described by

$$\Delta N(x_0, y_0) = K_n \Delta n_n(x_0, y_0) + K_i \Delta n_i(x_0, y_0) + K_e \Delta n_e(x_0, y_0) \quad (1),$$

where K is a relative refractive index, Δn is a density change, and subscripts n, i and e denote neutrals, ions and electrons, respectively. The laser intensity distribution of the Gaussian beam U_{G0} with a waist of W is given by

$$U_G(x_0, y_0) = U_{G0} \exp\left(-\frac{x_0^2+y_0^2}{W^2}\right) \quad (2).$$

When the Gaussian laser beam is transmitted through the arc region, the complex amplitude function of the laser beam on the incident x_0-y_0 plain is expressed by the following equation:

$$U_0(x_0, y_0) = U_G(x_0, y_0) \exp\{i\Delta\varphi(x_0, y_0)\} \quad (3),$$

where $\Delta\varphi(x_0, y_0) = (2\pi/\lambda)\Delta N_L(x_0, y_0)$ is a phase difference caused by $\Delta N_L(x_0, y_0)$. Here, ΔN_L indicates the integrated ΔN along the line of sight. The complex amplitude function of the laser beam on the x-y plain $U_f(x, y)$ is described under the paraxial approximation as follows:

$$U_f(x, y) = A' \int_{-\infty}^{\infty}\int_{-\infty}^{\infty} U_0(x_0, y_0) \exp\left\{-i2\pi\left(\frac{x_0}{f\lambda_0}x + \frac{y_0}{f\lambda_0}y\right)\right\} \quad (4),$$

where A' is an arbitrary constant, f is a focal length of the lenslets and λ_0 is the laser wavelength.

In order to estimate where the laser wavefront with spatial frequency λ [μm] is collected on the x-y plain, equation (4) was calculated for $\Delta\varphi(x_0, y_0) = \Delta\varphi_0 \cos(2\pi r_0/\lambda)$, where $\Delta\varphi_0$ is an arbitrary constant and r_0 is described by $r_0 = \sqrt{x_0^2+y_0^2}$ [mm]. By solving equation (4) under an actual focal length of f = 154 mm and laser wavelength of λ_0 = 404 nm in this study, the following relation was derived:

$$r = 6.1\times10^4/\lambda \text{ [μm]} \quad (r = \sqrt{x^2+y^2}) \quad (5).$$

This means that when the laser wavefront with a spatial frequency of λ = 100 μm, for example, is injected onto the incident lenslet, it is collected along the circular aperture with a radius of r = 610 μm. Since the spatial frequency of the turbulent gas density is transcribed onto the laser wavefront, the turbulent structure with a certain dimension is selectively visualized by the circular aperture with a specified radius. The optical configuration of the present Schlieren system is shown in Fig.2. In this study, various bandpass plates with different aperture radii were fabricated. While the widths of the circular apertures dr were fixed at dr = 100 μm, the aperture radii ranged from 150 μm to 3400 μm, which corresponded to

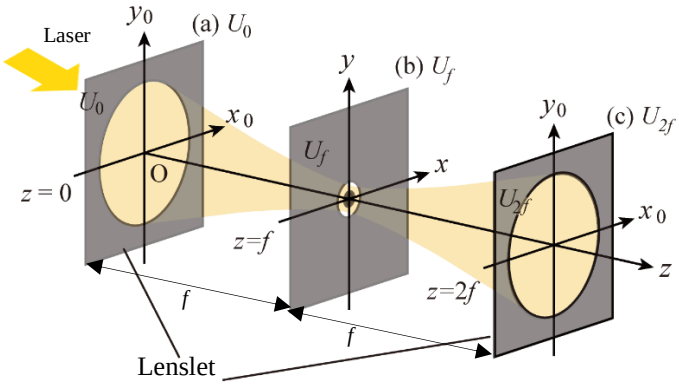

Fig.1. Bandpass spatial filter.

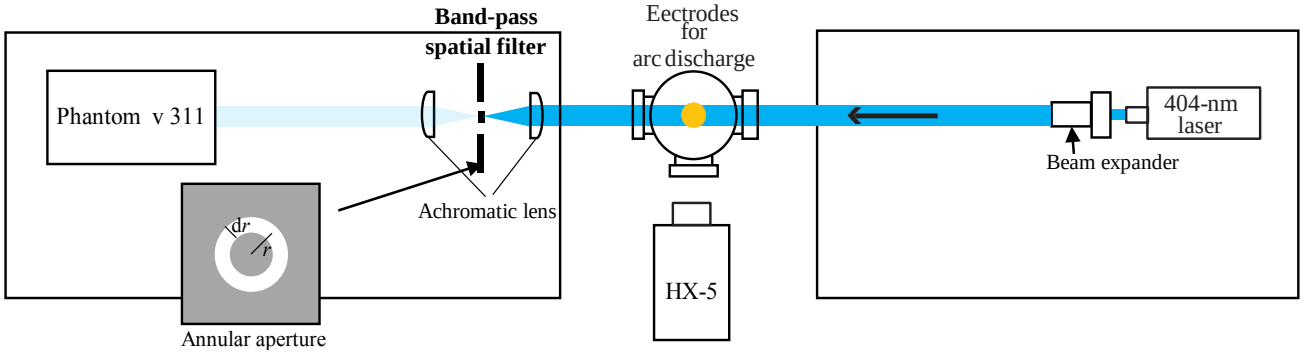

Fig.2. Optical system

the spatial frequency from 600 μm to 20 μm. The turbulent visualization was conducted by using high speed video camera (Vision Research Inc., Phantom v311) under a framing rate of 10000 fps and exposure time of 0.1 ms. The spatial resolution of the present Schlieren optics was 20 μm. The detailed description on the electron density imaging under strong turbulence is published elsewhere [8].

Fig.3 shows the schematic configuration of arc generation device. Arc discharges were established in a 50-mm gap between copper-tungsten electrodes confined by a gas flow nozzle. The nozzle was filled with arc-quenching gas media of air, CO_2 or SF_6 with atmospheric pressure. The nozzle throat was realized by a transparent cubic quartz cell with a dimension of $10\times10\times10mm^3$ was integrated with the gas flow nozzle for transmitting the laser beams through the arc plasma regions. A small current arc with DC 60 A was initially generated between the electrodes under a gas flow rate of 200L/min for air and CO_2 and 100L/min for SF_6. Subsequently, a half-wave current with an amplitude of 1400 A and frequency of 50 Hz was superimposed on the small current. The large current conduction induced fulfilment of the arc over the nozzle throat and caused the clogging of the blasted gas short of the nozzle throat inlet. As the large current decreased and approached current zero, the clogged gas flowed into the nozzle throat at high pressure above 0.1 MPa. The time at the natural current zero was defined as t = 0 μs in this study.

RESULTS AND DISCUSSION

Fig.4 shows a spatiotemporal evolution of the turbulent dynamics with a size of 33-43 μm, which were observed at t = -400, -300, -200, -100 and 0 μs for air blasted arcs; Fig.5, CO_2 blasted arcs; Fig.6, SF_6 blasted arcs. The instantaneous arc current values at t = -300, -200, -100 and 0 μs were 150, 100, 50 and 0 A, respectively. Notably, the light intensity in the lower region of Fig.4 does not demonstrate the turbulent dynamics and it was the stray light scattered by the deteriorated cubic quartz cell, which was thermally shocked in contact with the large current arc. A comparison of these images clearly shows that the SF_6 gas flow had even stronger turbulence compared with air and CO_2. Fig.6 shows that the turbulence with a size of 33-43 μm is not distributed randomly; rather, it is arranged circularly, which is seen like a hedgehog. The radii of the hedgehogs ranged from 1 to 5 mm. Therefore, it is suggested that the turbulence for the decaying SF_6 arc had a hierarchical structure, where the small turbulence in a size of ~10 μm formed millimeter-scale large circles. The combined structures of the small and large turbulence were also observed for the air and CO_2 blasted arcs.

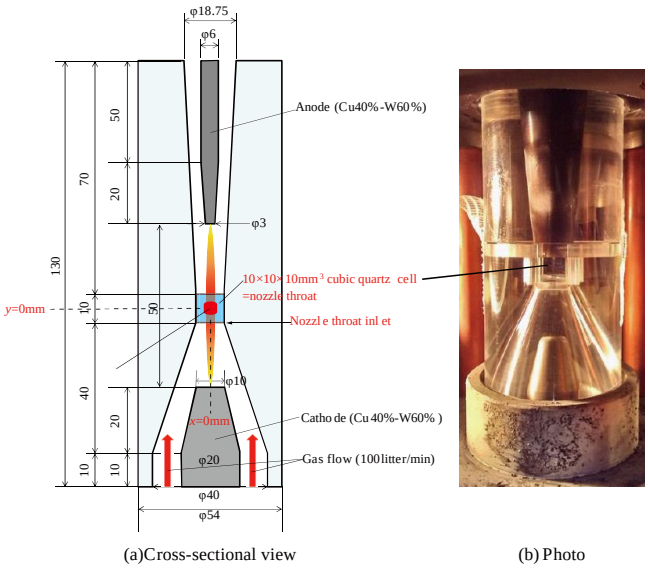

(a)Cross-sectional view (b) Photo

Fig.3. Gas flow nozzle for confinement of decaying arc.

The Kolmogorov scale is regarded as the minimum eddy size [15]. In analogous to the turbulence characteristics of a thermal plasma jet, the small turbulence observed in this study could demonstrate the entrained eddies of the blasted cold gas [16]. The minimum turbulent sizes for each quenching gas were measured by changing the radii of the circular apertures r. The parametric measurement demonstrated that the minimum turbulent sizes for air, CO_2 and SF_6 were 75, 45 and 30 μm, respectively. These minimum sizes of the small turbulence could correspond to the Kolmogorov scales and can be used for the determination of the temperature and/or the energy dissipation rate of the blasted cold gas. Further, the waist of the small turbulent distributions could demonstrate the entrainment of the blasted cold gas [16].

Fig.7 shows the time dependence of electron densities for air, CO_2 and SF_6 [17]. It should be noted that the electron densities were measured for a gas flow nozzle with a similar design to that of the present study. Each plot shows the arc core electron densities averaged along the axial direction y. Different plots at the same timings demonstrate the shot-to-shot variations. The electron density for SF_6 demonstrated the fastest decrease, which was followed by CO_2 and air. This order was consistent with the previous research on the dielectric recovery time constants of the three kinds of arc-quenching gas media [18]. The strongest small turbulence of SF_6 could cause the cold gas mixing into the arc, which resulted in the rapid arc cooling and the fastest electron density reduction. These experimental results on the turbulent structures and electron density decaying behavior are quite useful for constructing a complete simulation model implementing the turbulent dynamics and finally, developing the eco-friendly gas circuit breakers using the SF_6-alternative gases.

CONCLUSION

Multi-directional turbulent structures visualized by specialized Schlieren method demonstrated hierarchical formations, where the small turbulence in sizes of ~10 μm were distributed along millimeter-scale large circles. The minimum sizes of the small turbulence could correspond to the Kolmogorov scales and they were 75, 45 and 30 μm for air, CO_2 and SF_6, respectively. The small turbulence in dimensions of 33-43 μm was even stronger for SF_6, compared with air and CO_2. Further, the electron density for SF_6 demonstrated the fastest decrease, which was followed by CO_2 and air. These experimental results on the turbulent and electron density behavior suggested that the strongest small turbulence of SF_6 could cause the cold gas entrainment into the arc, which resulted in the rapid arc cooling and the fastest electron density reduction.

Acknowledgments

The authors like to thank Prof. Katsumi Suzuki of Tokyo Denki University and Prof. Takeshi Shinkai of Tokyo University of Technology for their support during this work.

REFERENCES

[1] L.G. Christophorou and R.J.V. Brunt, 1995, "SF_6/N_2 mixtures: basic and HV insulation properties", *IEEE Trans. Dielectr. Electr. Insul.* vol. 2, 952–1003.

[2] M.T.C. Fang and W.Y. Lin, 1990, "Current zero behaviour of a gas-blast arc. Part 1: nitrogen", *IEE Proc. A* vol. 137, 175–183.

[3] Y. Yokomizu, T. Sakuta and Y. Kito, 1989, "A novel approach to AC air arc interruption phenomena viewed from the electron density at current zero", *J. Phys. D: Appl. Phys.* vol. 22, 129–135.

[4] Y. Kito, T. Sakuta, M. Kurono and T. Saiki, 1987, "Influences of copper vapor contamination on temperature distribution profile in air blasted arc columns", *IEEJ Trans. Power Energy* vol. 107-A, 127–134 (in Japanese).

[5] Y. Inada, A. Kumada, H. Ikeda, K. Hidaka, T. Nakano, K. Murai, Y. Tanaka and T. Shinkai, 2017, "Comparative study on extinction process of gas-blasted air and CO_2 arc discharge using 2D electron density imaging sensor", *J. Phys. D: Appl. Phys.* vol. 50, 175202.

[6] Y. Tanaka and K. Suzuki, 2013, "Development of a chemically nonequilibrium model on decaying SF_6 arc plasmas", *IEEE Trans. Power Deliv.* vol. 28, 2623–2629.

[7] H. Sun, Y. Tanaka, K. Tomita, Y. Wu, M. Rong, Y. Uesugi and T. Ishijima, 2016, "Computational non-chemically equilibrium model on the current zero simulation in a model N_2 circuit breaker under the free recovery condition", *J. Phys. D: Appl. Phys.* vol. 49, 055204.

[8] Y. Inada, H. Nagai, S. Yamaguchi, A. Kumada, H. Ikeda, K. Hidaka, T. Nakano, Y. Tabata, Y. Demura, Y. Tanaka, T. Shinkai and M. Maeyama, 2018, "Spatial-filter-installed Shack–Hartmann sensor for two-dimensional electron density visualization of SF6 arc discharge under strong turbulent flow", *J. Phys. D: Appl. Phys.* vol. 51, 345203.

[9] N.P.T. Basse, R. Bini and M. Seeger, 2009, "Measured turbulent mixing in a small-scale circuit breaker model", *Appl. Opt.* vol. 48, 6381-6391.

[10] B. Ineichen, U. Kogelschatz and R. Dändliker, 1973, "Schlieren diagnostics and interferometry of an arc discharge using pulsed holography", *Appl. Opt.* vol. 12, 2554–2556.

[11] U. Kogelschatz, 1974, "Application of a simple differential interferometer to high current arc discharges", *Appl. Opt.* vol. 13, 1749–1752.

[12] G.S. Settles, 2006, *Schlieren and Shadowgraph Techniques*, Springer-Verlag, Berlin, Germany, 221-229.

[13] G.S. Settles, 2006, *Schlieren and Shadowgraph Techniques*, Springer-Verlag, Berlin, Germany, 32-37.

[14] H. Stark (ed), 1982, *Application of Optical Fourier Transforms*, Academic, London, UK, 4-7.

[15] M. Shigeta, 2016, "Turbulence modelling of thermal plasma flows", *J. Phys. D: Appl. Phys.* vol. 49, 493001.

[16] E. Pfender, J. Fincke and R. Spores, 1991, "Entrainment of cold gas into thermal plasma jets", *Plasma Chem. Plasma Process.* vol. 11, 529–543.

[17] Y. Inada, H. Nagai, A. Kumada, H. Ikeda, K. Hidaka, T. Nakano, Y. Tabata, Y. Tanaka and M. Maeyama, 2018, "Comparative Study on High-Current Arc Extinction Process under Air, CO_2 and SF_6 Gas Blasting Using Two-Dimensional Electron Density Visualisation System", *Proceedings of GD conference*, A25, vol.1, 143-146

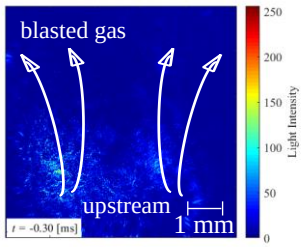

(a) t = -300μs

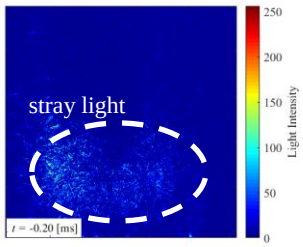

(b) t = -200μs

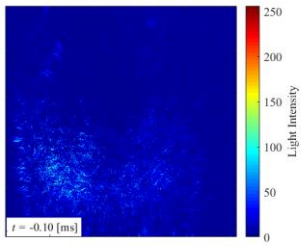

(c) t = -100μs

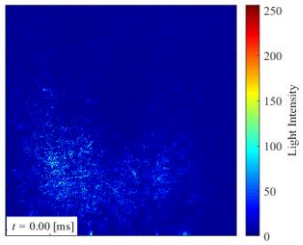

(d) t = 0μs

Fig.4. Spatiotemporal evolution of turbulent dynamics for air.

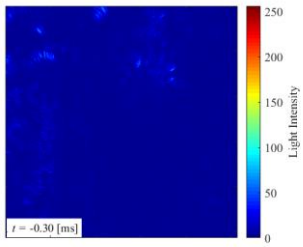

(a) t = -300μs

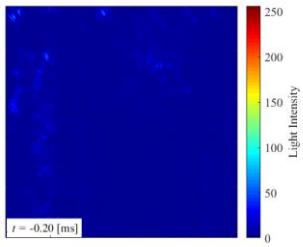

(b) t = -200μs

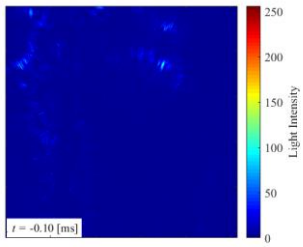

(c) t = -100μs

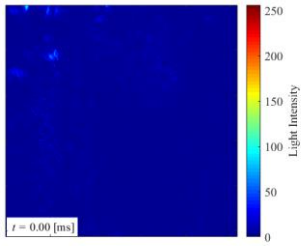

(d) t = 0μs

Fig.5. Spatiotemporal evolution of turbulent dynamics for CO_2.

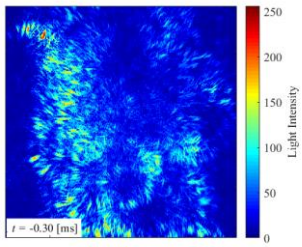

(a) t = -300μs

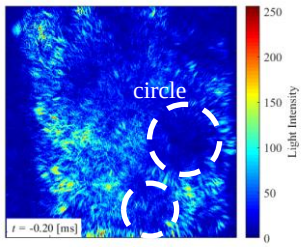

(b) t = -200μs

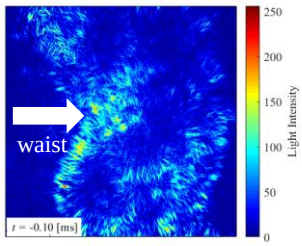

(c) t = -100μs

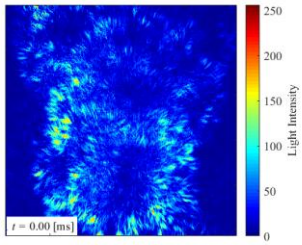

(d) t = 0μs

Fig.6. Spatiotemporal evolution of turbulent dynamics for SF_6.

[18] T. Nakano, Y. Tanaka, K. Murai, Y. Uesugi, T. Ishijima, K. Tomita, K. Suzuki and T. Shinkai, 2017, "Evaluation of arc quenching characteristics of various gases using power semiconductors", *J. Phys. D: Appl. Phys.* vol. 50, 485602.

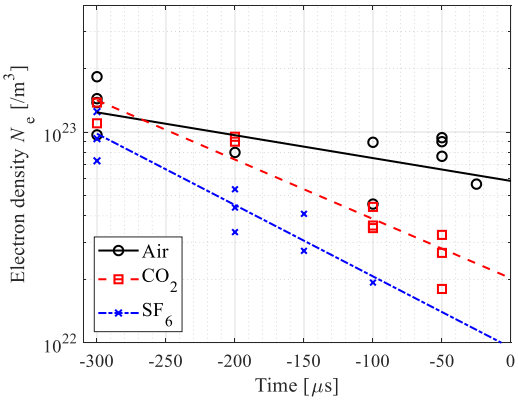

Fig. 7. Time dependence of electron density in nozzle throat under air, CO_2 and SF_6 gas blasting.